Structural and Functional Analysis of the Pyocyanin Biosynthetic Protein PhzM from *Pseudomonas aeruginosa*[†,‡]

James F. Parsons,*[,§] Bryan T. Greenhagen,[§] Katherine Shi,[§] Kelly Calabrese,[§] Howard Robinson,[||] and Jane E. Ladner*[,§,⊥]

Center for Advanced Research in Biotechnology, University of Maryland Biotechnology Institute, National Institute of Standards and Technology, 9600 Gudelsky Drive, Rockville, Maryland 20850, and Biology Department, Brookhaven National Laboratory, Upton, New York 11973-5000

Received November 27, 2006; Revised Manuscript Received December 16, 2006

ABSTRACT: Pyocyanin is a biologically active phenazine produced by the human pathogen *Pseudomonas aeruginosa*. It is thought to endow *P. aeruginosa* with a competitive growth advantage in colonized tissue and is also thought to be a virulence factor in diseases such as cystic fibrosis and AIDS where patients are commonly infected by pathogenic Pseudomonads due to their immunocompromised state. Pyocyanin is also a chemically interesting compound due to its unusual oxidation−reduction activity. Phenazine-1-carboxylic acid, the precursor to the bioactive phenazines, is synthesized from chorismic acid by enzymes encoded in a seven-gene cistron in *P. aeruginosa* and in other Pseudomonads. Phenzine-1-carboxylic acid is believed to be converted to pyocyanin by the sequential actions of the putative *S*-adenosylmethionine-dependent *N*-methyltransferase PhzM and the putative flavin-dependent hydroxylase PhzS. Here we report the 1.8 Å crystal structure of PhzM determined by single anomalous dispersion. Unlike many methyltransferases, PhzM is a dimer in solution. The 36 kDa PhzM polypeptide folds into three domains. The C-terminal domain exhibits the α/β-hydrolase fold typical of small molecule methyltransferases. Two smaller N-terminal domains form much of the dimer interface. Structural alignments with known methyltransferases show that PhzM is most similar to the plant *O*-methyltransferases that are characterized by an unusual intertwined dimer interface. The structure of PhzM contains no ligands, and the active site is open and solvent-exposed when compared to structures of similar enzymes. In vitro experiments using purified PhzM alone demonstrate that it has little or no ability to methylate phenzine-1-carboxylic acid. However, when the putative hydroxylase PhzS is included, pyocyanin is readily produced. This observation suggests that a mechanism has evolved in *P. aeruginosa* that ensures efficient production of pyocyanin via the prevention of the formation and release of an unstable and potentially deleterious intermediate.

Pyocyanin is a chemically fascinating and biologically important pigmented secondary metabolite produced by the human pathogen *Pseudomonas aeruginosa*. Pyocyanin and other phenazines are virulence factors produced by *P. aeruginosa* and other Pseudomonads (*1*). While healthy individuals are rarely infected by *P. aeruginosa*, the organism is a constant threat to those with conditions such as cystic fibrosis, AIDS, and other immune disorders, as well as those requiring long-term hospitalization. Approximately 10% of the estimated 2 million cases of nosocomial infection reported each year are caused by *P. aeruginosa*, and for many patients the prognosis is poor once infection is established. Mortality rates range from 20 to 70% depending on underlying conditions. Many virulence factors, including antibiotic resistance, contribute to the difficulty in controlling *P. aeruginosa* infections (*2*−*5*). Recently, phenazines have been recognized as contributing to the virulence of this organism as well. Pyocyanin is the principal phenazine produced by *P. aeruginosa*, and it has been shown to contribute to the unusual persistence of *P. aeruginosa* infections (*6*). Pyocyanin is toxic largely due to its ability to engage in oxidation−reduction reactions that deplete cells of NADH, glutathione, and other antioxidants. The redox activity of pyocyanin generates oxidants such as superoxide and peroxides. These pyocyanin-associated reactive oxygen species have been linked to various cellular phenomena that enhance the ability of *P. aeruginosa* to survive (*5*).

[†] This work was supported by NIH Grant AI067530 (J.F.P.). Some data for this study were measured at beamline X29 if the National Synchroton Light Source. Financial support comes principally from the Offices of Biological and Environmental Research and of Basic Energy Sciences of the US Department of Energy, and from the National Center for Research Resources of the National Institutes of Health.

[‡] Coordinates for PhzM have been deposited in the RCSB Protein Data Bank as entry 2IP2.

* To whom correspondence should be addressed: Center for Advanced Research in Biotechnology, 9600 Gudelsky Dr., Rockville, MD 20850. Phone: (240) 314-6158. Fax: (240) 314-6255. E-mail: parsonsj@umbi.umd.edu (J.P.), ladner@umbi.umd.edu (J.L.).

[§] Center for Advanced Research in Biotechnology.

[||] Brookhaven National Laboratory.

[⊥] National Institute of Standards and Technology.

[1] Abbreviations: PCA, phenazine-1-carboxylate; ADIC, 2-amino-2-deoxyisochorismate; DHHA, *trans*-2,3-dihydro-3-hydroxyanthranilic acid; 1-HP, 1-hydroxyphenazine; IOMT, isoflavone *O*-methyltransferase from alfalfa; 5-Me-PCA, 5-methylphenazine-1-carboxylate; MS, mass spectrometry; DTT, dithiothreitol; EDTA, ethylenediaminetetraacetic acid; PEG, polyethylene glycol; TEV, tobacco etch virus; SAM, *S*-adenosylmethionine; SAH, *S*-adenosylhomocysteine; SAD, single-wavelength anomalous dispersion.

10.1021/bi6024403 CCC: $37.00
Published on Web 01/25/2007

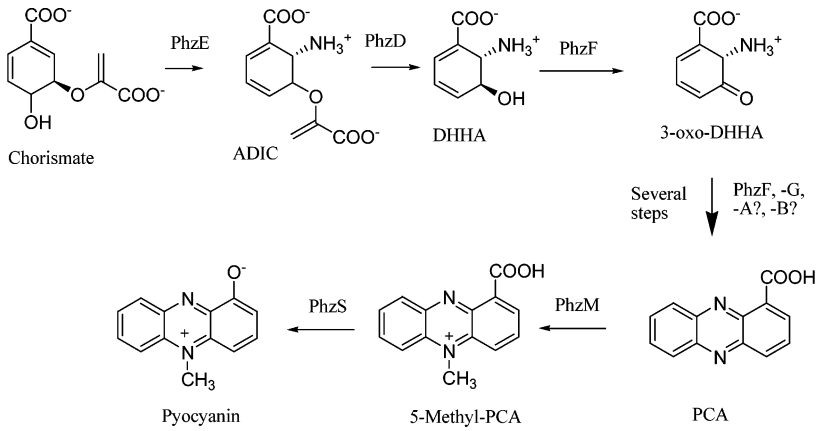

FIGURE 1: Proposed biosynthetic pathway leading to pyocyanin in *P. aeruginosa*.

Phenazine-1-carboxylic acid (PCA)[1] is synthesized by *P. aeruginosa* from chorismic acid by the enzymes encoded on two nearly identical seven-gene *phzABCDEFG* operons (*7*). Recently, significant progress has been made in understanding the biochemistry of PCA production. PhzE is an anthranilate synthase homologue that produces 2-amino-2-deoxyisochorismate (ADIC) from chorismate (Figure 1). PhzD is a hydrolase that produces *trans*-2,3-dihydro-3-hydroxyanthranilic acid [DHHA (*8*)]. PhzF then catalyzes an epimerization and perhaps facilitates the dimerization reaction that yields the initial tricyclic ring system (*9*, *10*). PhzA, -B, and -G are believed to be involved in the oxidation/aromatization of the initial tricyclic species (*9*). Previous data indicate, however, that they are not strictly required for PCA production as PhzF alone was shown to produce PCA from DHHA, albeit slowly (*9*, *10*). Crystal structures of PhzD, -F, and -G are available and have contributed significantly to the understanding of the mechanisms involved in PCA biosynthesis (*8*−*11*).

Little is known, however, about the conversion of PCA to pyocyanin. It has been postulated to be a two-step process involving N-methylation by PhzM and hydroxylation by PhzS (*12*). Such a scenario, however, would produce, as an intermediate, the highly reactive and unstable compound 5-methylphenazine-1-carboxylate (5-Me-PCA) (*13*). While PhzS can act on PCA, producing 1-hydroxyphenazine [1-HP (*12*)], this compound was demonstrated using in vitro assays and isotopic labeling not to be a precursor to pyocyanin (*14*, *15*), indicating that PhzM acts before PhzS in pyocyanin biosynthesis. To better understand how PCA is converted to pyocyanin, we report the crystal structure of PhzM at 1.8 Å. The structure indicates that PhzM indeed has the methyltransferase fold and that it is surprisingly similar to a family of plant *O*-methyltransferases exemplified by isoflavone *O*-methyltransferase [IOMT (*16*)]. PhzM, like the plant enzymes, has an N-terminal dimerization domain that not only forms an extensive intertwined interface but also contributes elements of the substrate binding site of the opposite subunit. Biochemical analysis has further revealed that, alone, PhzM has no detectable activity toward PCA. Pyocyanin is readily produced, however, when PhzS and NADH are present. Isolation of either PhzM or PhzS inside a dialysis membrane results in no pyocyanin formation, suggesting that an at least transient physical interaction between PhzM and PhzS is required to activate production of pyocyanin.

MATERIALS AND METHODS[2]

Cloning. DNA fragments encoding the *P. aeruginosa* PhzM and PhzS proteins were amplified from *P. aeruginosa* genomic DNA (ATCC) using synthetic primers compatible with the published DNA sequences (*12*). Also, in the case of *phzM*, DNA encoding a tobacco etch virus (TEV) protease cleavage site was included upstream of the *phzM* start codon. *Nde*I and *Hin*dIII restriction enzyme sites were included in the primers, and the digested fragments were ligated into the similarly digested expression vector pET28a (Novagen), yielding the constructs pET28-TEV-*phzM* and pET28-*phzS*.

Protein Expression and Purification. *P. aeruginosa* PhzM was expressed in *Escherichia coli* strain BL21(DE3)Gold. Cells harboring the pET28a-TEV-*phzM* plasmid were grown in shaker flasks at 37 °C in LB medium containing 100 μg/mL kanamycin. Isopropyl β-D-thiogalactopyranoside was added to the culture (final concentration of 1 mM) when the culture density reached an optical density of 0.8 at 600 nm. Cells were harvested after 3 h and lysed by sonication in 50 mM KH_2PO_4 and 300 mM NaCl (pH 8.0). PhzM was purified by cobalt affinity chromatography as directed by the resin manufacturer (Sigma). Fractions containing pure PhzM were pooled and dialyzed against 50 mM Tris, 0.1 mM EDTA, and 1 mM DTT (pH 7.6) and concentrated to ~10 mg/mL. TEV protease was added to a final concentration of ~50 μg/mL, and the mixture was incubated at 28 °C overnight. TEV protease (also His-tagged) and undigested PhzM were removed by a second passage over the affinity column. Pure, cleaved PhzM was then dialyzed against 50 mM MOPS, 1 mM DTT, and 0.1 mM EDTA (pH 7.0), concentrated to ~15 mg/mL, and stored at −80 °C. The yield was ~70 mg of pure enzyme/L of culture. Selenomethionine-labeled PhzM was expressed in *E. coli* strain B834(DE3) by growing the bacteria in M9 minimal medium supplemented with selenomethionine. Purification was conducted as described above.

PhzS was expressed in a similar manner, but the histidine affinity tag was removed using human thrombin (Haematologic Technologies). Thrombin (10 μg/mL) was added to

[2] Certain commercial materials, instruments, and equipment are identified in this manuscript to specify the experimental procedure as completely as possible. In no case does such identification imply a recommendation or endorsement by the National Institute of Standards and Technology, nor does it imply that the materials, instruments, or equipment identified is necessarily the best available for the purpose.

Table 1: Data Collection Statistics

	native	SeMet
space group	*P*1	*P*1
cell parameters (*a*, *b*, *c*) (Å)	46.97, 62.41, 68.75	47.34, 62.53, 69.35
cell parameters (α, β, γ) (deg)	97.47, 105.37, 108.09	97.17, 105.82, 108.25
wavelength of data collection (Å)	1.541	0.9791
no. of measured intensities	447399	52133
no. of unique reflections	60747	19336
resolution of data (Å)	29.4−1.8	30.0−2.6
highest-resolution shell (Å)	1.86−1.80	2.69−2.60
R_{sym} (overall/high-resolution shell)	0.110/0.371	0.093/0.214
completeness (%) (overall/high-resolution shell)	94.2/90.7	89.6/57.7
redundancy (overall/high-resolution shell)	7.36/7.31	2.8/2.2
mean I/σ (overall/high-resolution shell)	11.3/2.6	20/10

∼15 mg/mL PhzS, and the mixture was incubated at room temperature for 6 h. After a second passage over the cobalt affinity column to remove any undigested protein, PhzS was dialyzed against 50 mM Bis-Tris (pH 6.5) and 1 mM DTT, concentrated to 21 mg/mL, and stored at −80 °C.

Molecular Mass from Laser Light Scattering. The solution molecular masses of PhzM and PhzS were determined by a combination of laser light scattering and interferometric refractometry using a DAWN EOS and Optilab DSP system (Wyatt). Samples were subjected to gel filtration chromatography (Shodex KW-803; 300 mm × 8 mm) prior to in-line analysis. Molecular masses were calculated using ASTRA. The column was typically equilibrated with 10 mM Tris (pH 7.5), 100 mM NaCl, and 0.1 mM EDTA. *S*-Adenosylmethionine (SAM; final concentration of 0.1 mM), NADH (0.2 mM), and PCA (0.4 mM) were included for experiments aimed at detecting a PhzM−PhzS complex.

Crystallization. Crystals of PhzM were grown at room temperature by the sitting drop vapor diffusion method. The well solution was 0.10 M MOPS (pH 7.0), 0.10 M magnesium chloride, and 20% (w/v) PEG 3350. Four microliter drops were made by adding equal volumes of protein solution and well solution. The protein concentration was typically ∼15 mg/mL before mixing. Crystals reached their maximum size in 2−3 days.

Data Collection. Diffraction data for the native structure were collected using a Rigaku Micro Max 007 rotating anode generator with an RAXIS IV^{++} detector (Rigaku/MSC, The Woodlands, TX). The crystal was cooled to 105 K with an X-stream 2000 Cryocooler (Rigaku/MSC) and was cryoprotected by covering the sitting drop with paraffin oil and pulling the loop-mounted crystal through the oil. SAD diffraction data for the selenomethionine-containing protein were collected at Brookhaven National Laboratory on beamline X29 using a wavelength of 0.9791 Å. Diffraction data were collected using a Rigaku Micro Max 007 rotating anode generator and a Rigaku RAXIS IV^{++} detector. The crystals were cooled to 105 K with an Oxford Cryosystems cryocooler and were cryoprotected by the addition of 50% PEG 4000 to the reservoir solution at a ratio of 1:1. Diffraction data in both cases were processed with CrystalClear/d*Trek (*17*). Statistics for the data collection are given in Table 1.

Table 2: Refinement Statistics

resolution limits (Å)	20.0−1.8
no. of reflections used	57471
R-factor (overall/high-resolution shell)	0.194/0.296
R_{free} (overall/high-resolution shell)	0.247/0.380
no. of water molecules	512
rms deviation for bond lengths (Å)	0.020
rms deviation for angles (deg)	1.74
average *B* for main chain/side chain/water (Å^2)	30.6/33.2/39.9

Structure Determination. The Matthews coefficient (2.52) indicated that there were two molecules in the unit cell. The presence of noncrystallographic 2-fold symmetry was also seen in the analysis of the data with XPREP (Bruker). Using the SAD data for the selenomethionine protein, 20 selenium sites were found by SHELXD and the hand of the sites was examined using SHELXC (*18*). The sites were then used in SOLVE/RESOLVE (*19*) to produce an electron density map that upon inspection using XTALVIEW appeared to be excellent. Using the iterative script SOLVE (www.solve.lanl.gov) which includes cycles of density modification and automated model building by RESOLVE and molecular refinement by REFMAC5 (*20*), 563 of the 668 residues were built and 206 side chains were placed. The pieces of this model were consolidated into the two chains for the two molecules in the unit cell using XTALVIEW. Then the native data were used, and the model was completed and refined by using XTALVIEW for adjusting and expanding the model and REFMAC5 for refining between building sessions. The final statistics are given in Table 2. The final model includes residues 5−334 for both polypeptide chains. The side chains of 21 residues in the A chain and 13 residues in the B chain were modeled in multiple conformations. There are other residues on the outside of the molecule that have less than optimal density for the side chain atoms, but the backbone is in good density for the entire model. In a Ramachandran plot, 93.4% of the residues fall into the most favorable regions and 6.6% fall into the additional allowed regions.

Analysis of Enzymatic Activities. Analytical reagents were typically obtained from Sigma. PCA was purified form cultures of *Pseudomonas fluorescens* according to the method of Gurusiddaiah et al. (*21*). 1-Hydroxyphenazine (1-HP) was purchased from TCI America. Authentic pyocyanin was produced by photo-oxidative hydroxylation of phenazine methosulfate [Sigma (*22*)].

Reactions that included PhzM and PhzS were typically conducted in 50 mM Tris (pH 7.8), 100 mM KCl, 0.5 mM SAM, and 0.5 mM NADH and were carried out at room temperature (∼22 °C). Pyocyanin production was analyzed by quenching reactions with KOH and extracting formed pyocyanin with methylene chloride. At high pH, the PCA substrate remains in the aqueous phase and does not interfere with subsequent analyses. PCA consumption was quantitated at 370 nm (ϵ = 19 000 M^{-1} cm^{-1}) after acidified reaction mixtures had been extracted with hexane, a procedure that leaves pyocyanin in the aqueous phase. Pyocyanin concentrations were determined spectrophotometrically at 387 nm (ϵ = 21 800 M^{-1} cm^{-1}) or 690 nm (ϵ = 4210 M^{-1} cm^{-1}). Pyocyanin formation could also be monitored continuously at 690 nm. SAM utilization was analyzed by HPLC as

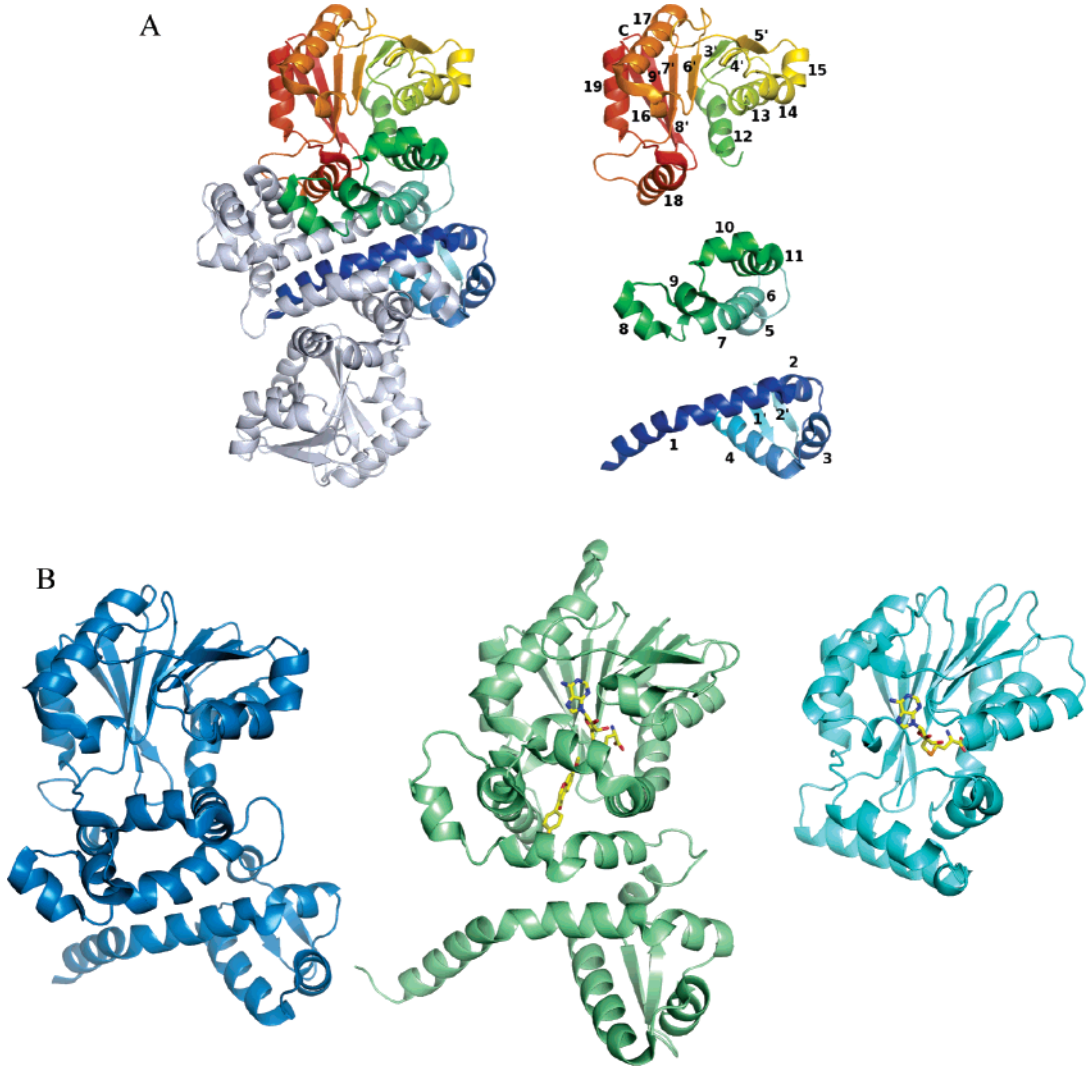

FIGURE 2: Structure of the PhzM dimer, illustration of the secondary structural elements of PhzM, and a comparison of the PhzM monomer with representative methyltransferases. (A) The PhzM dimer, with one subunit colored like a rainbow and the other colored gray. Secondary structure diagram of the PhzM monomer separated by domain and colored as in the dimer. Helices are numbered 1−18, and strands are numbered 1′−9′. (B) Ribbon diagrams comparing the structure of PhzM (left) with those of a structural homologue (IOMT), and a typical monomeric small molecule methyltransferase, YecO, from *Heamophilus influenzae*.

described below. PhzS-dependent conversion of PCA to 1-HP was analyzed spectrophotometrically and by HPLC. 1-HP was identified by comparing its absorption spectra and retention time to those of authentic 1-HP. The apparent rate of 1-HP formation was determined by monitoring its formation at 460 nm ($\epsilon = 760\ M^{-1}\ cm^{-1}$).

Equilibrium dialysis chambers were used to assess substrate utilization and product formation upon incubation of PCA with PhzM, PhzS, or both and all necessary cofactors. Chambers holding a total of 350 μL were assembled with an 8000 molecular weight cutoff dialysis membrane dividing the chamber in two halves. Experiments were conducted with PhzM and PhzS on different sides, and control experiments were conducted with both enzymes on the same side. Overnight incubations were carried out at room temperature with gentle shaking. Reactions were analyzed by UV−visible spectrophotometry or by HPLC. Larger-scale reactions were also conducted to better ensure that oxygen depletion was not a concern. Three 25 mL reactions were assembled in 50 mL tubes to allow aeration by gentle shaking. Either PhzM, PhzS, or NADH (control) was placed in a 3 cm section of a 10 mm flat width sealed dialysis membrane and placed inside the tube. Tubes were incubated as described above.

Filtration assays were conducted by incubating reaction mixtures lacking either PhzM or PhzS for various times and then passing the mixture through a 10 kDa molecular mass cutoff centrifugal filter (Millipore) to remove the enzyme that was added. The initially excluded enzyme was then added to the flow-through, and the solution was analyzed for product formation.

Instrumental Methods. UV−visible spectra were acquired at 25 °C using a Cary 4 double-beam spectrophotometer. HPLC was used to separate and identify reaction products on the basis of retention time. A 4.6 mm × 150 mm μbondapak C18 reversed phase column (Waters) was used in conjunction with a Gilson binary gradient HPLC system. The separation method was similar to that described previously (*12*) except the aqueous phase was 1% acetic acid. The flow rate used was 1 mL/min, and analytical injections were ≤20 μL.

Table 3: Results of a MATRAS Search for Proteins Similar to PhzM

PDB entry	protein	MATRAS R_{dis} similarity score[a]	rmsd (Å) for aligned Cα atoms	no. of aligned residues	% sequence identity
1KYW	CaOMT, alfalfa	58.8	2.9	313	24
1FP2	IOMT, alfalfa	55.6	3.7	319	25
1FP1	ChOMT, alfalfa	55.7	2.7	308	21
1TW3	DnrK, *Streptomyces peucetius*	57.6	4.1	321	27
1ZG3	isoflavonone MT, alfalfa	52.8	3.7	235	27
1X19	BchU, *Chlorobium tepidum*	50.8	3.4	315	17
1QZZ	Rdmb, *Streptomyces purpurascens*	44.8	6.7	321	24
1IM8[b]	YecO, *Heamophilus influenzae*	28.2	3.3	194	15

[a] See http://biunit.naist.jp/matras/index.html for a detailed description of scoring. [b] Included to illustrate the reduction in similarity beyond the closer homologues.

RESULTS

Overall Structure. PhzM, unlike the majority of structurally characterized small molecule methyltransferases (*23*), is a dimer (Figure 2A). Each polypeptide is made up of three domains (Figure 2A). The N-terminal domain (domain I, residues 1−97) is the dimerization domain and contains four helices and one small β-sheet of two four-residue strands. Domain II is made up of residues 98−168 and is all helical. The C-terminal domain (domain III, residues 169−334) of PhzM has a structure typical of most small molecule methyltransferases, many of which have been characterized structurally. Domain III contains the SAM binding site, has a Rossmann-like fold, and consists of a β-sheet with the strand topology 3214576 with the seventh strand antiparallel to the other strands. There are eight helices in this domain. Seven of these helices flank the central β-sheet to form the typical $\alpha\beta\alpha$ sandwich, and helix 7 of this domain (helix 18 of the polypeptide) is involved in the dimer interface, forming hydrogen bonds with the side chains of helix 4 and hydrophobic interactions with helix 1 of the second polypeptide of the dimer.

Dimer Interface. The molecule forms a dimer with an extensive interface that buries 30% or 4100 Å^2 of the surface area of each monomer (Figure 2A). The interface is formed primarily by domain I but also includes α18 from domain III. The N-terminal helix (α1) of PhzM defines one wall of the active site of the opposing subunit. Laser light scattering confirms that PhzM is a dimer in solution as well with a molecular mass of 73 550 ± 490 Da for PhzM, roughly twice the calculated monomer mass of 36 226 Da.

Structure Relatives. The fold of the PhzM SAM binding domain (domain III) categorizes PhzM as a class I methyltransferase (*23*). Four other classes have been described (classes II−V), all having far fewer members with known structures than the well-characterized class I. Convergent evolution has been credited for the diversity that is seen (*23*). Automated superposition of the refined PhzM structure using MATRAS (*24*) revealed that seven other methyltransferases (among >50 unique methyltransferases in the structural database) exhibit the same unusual dimer interface seen in PhzM. This feature distinguishes these enzymes from the majority of methyltransferases. The data in Table 3 show that the PhzM homologues are a curious mix of plant and bacterial methyltransferases. It is probable, however, on the basis of protein sequence analysis, that the fold is quite common in both plants and bacteria and that more structures will be forthcoming.

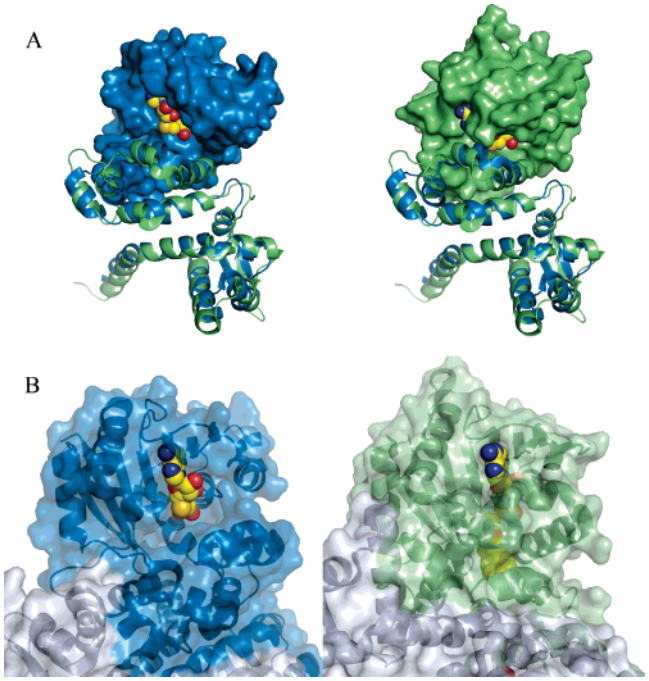

FIGURE 3: Surface representations illustrating the solvent-exposed state of the PhzM active site. (A) Superposition of PhzM and IOMT. In both panels, domains 1 and 2 were aligned and are shown as blue (PhzM) and green (IOMT) ribbons to indicate clearly that the viewing angle is identical in each panel. In the left panel, the surface of domain 3 of PhzM only is shown along with SAH from IOMT. In the right panel, the surface of domain 3 of IOMT is shown along with bound SAH. (B) Portions of the PhzM structure (left) with a model of SAH in the active site and IOMT (right) in complex with products shown with transparent surfaces. Modeled or bound ligands are shown as space-filling spheres.

Active Site. The active site of PhzM is located in domain 3 at the C-terminal ends of the first two β-strands of the large β-sheet (β3 and β4 in Figure 2). PhzM possesses the highly conserved DVGGGXG motif (residues 173−179) that defines the SAM binding site of methyltransferase enzymes, suggesting that PhzM does indeed function as a methyltransferase. PhzM is one of few methyltransferases in the structural database that is unliganded however. Typically, methyltransferases readily crystallize with either SAM or *S*-adenosylhomocysteine (SAH; the spent cosubstrate) in the active site. SAH in most cases binds more tightly than SAM (*25*). Frequently, structures are obtained with the methyl accepting substrate or product as well. Figure 3, however, illustrates the degree to which the PhzM active site is exposed to solvent compared to the active site of IOMT with SAH bound. The openness of the PhzM active site appears to be

Table 4: Summary of Results from in Vitro Assays of PhzM and PhzS

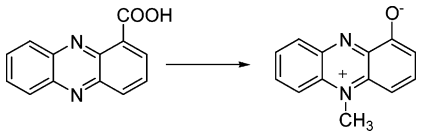

component excluded from the assay[a]	result
none	pyocyanin formed, apparent k_{cat} of 1.3 s^{-1}
PhzS	no activity[b]
PhzM	1-HP formed, apparent k_{cat} of 0.03 s^{-1}
NADH	no activity[b]
SAM	1-HP formed, apparent k_{cat} of 0.03 s^{-1}
PCA	no activity[b]

[a] The assay included 1 μM PhzM, 1 μM PhzS, 0.5 mM SAM, 0.4 mM PCA, and 1 mM NADH. [b] No detectable SAM consumption in 4 h. See the text for additional details.

related to the orientation of the domains in PhzM relative to each other. When PhzM and IOMT are superimposed, either domains 1 and 2 or domain 3 of each protein can be superimposed with an rmsd of 2−2.5 Å. A slight rotation of the first helix in domain 3 (α12, Figure 2A) of PhzM appears to throw the alignment off for the remaining domain(s) where corresponding Cα atoms deviate by >7 Å.

Without bound ligands, it is difficult to speculate about the identity of residues that may be involved in binding of the methyl acceptor substrate or in catalysis; however, proximity and orientation effects may dominate in chemical reactions catalyzed by PhzM rather than there being particular residues that play indispensable roles (see Discussion).

In Vitro Activity of PhzM and PhzS. To confirm the proposed roles of PhzM and PhzS in pyocyanin biosynthesis, the enzymatic activity of each was investigated. Table 4 summarizes the following results. Incubations of PhzM with its presumed substrates, PCA and SAM, yielded no detectable product, and substrate concentrations were unchanged after extended incubations. SAM consumption was monitored by HPLC, and PCA consumption was followed spectrophotometrically at 370 nm or by HPLC. A wide range of reaction conditions were screened. pH, ionic strength, substrate concentrations, divalent cations, and other factors were varied, but no condition resulted in PhzM activity. Assays of crude lysates containing overexpressed PhzM also indicated the enzyme was inactive.

Analysis of PhzS alone was complicated by the fact that its presumed substrate, 5-Me-PCA, is the product of the PhzM reaction. Literature reports (*13*) suggest 5-Me-PCA is both unstable and possibly an intermediate in more than one process, either of which would be compelling reasons for PhzM to be under some form of regulatory control.

The literature further suggests that PCA is also a substrate for PhzS and that it is converted to 1-HP. This was confirmed by incubating PhzS with PCA and NADH. 1-HP was formed in a NADH-dependent manner with an apparent k_{cat} of 0.03 s^{-1} in our assay. Consumption of NADH was evident in monitoring decay at 340 nm in a continuous assay containing PCA and NADH. There were indications, however, that PCA is a poor substrate for PhzS as complete conversion of PCA to 1-HP was not obtained and more NADH was consumed than the amount of 1-HP produced. This observation suggests that PCA is uncoupling flavin reduction from substrate

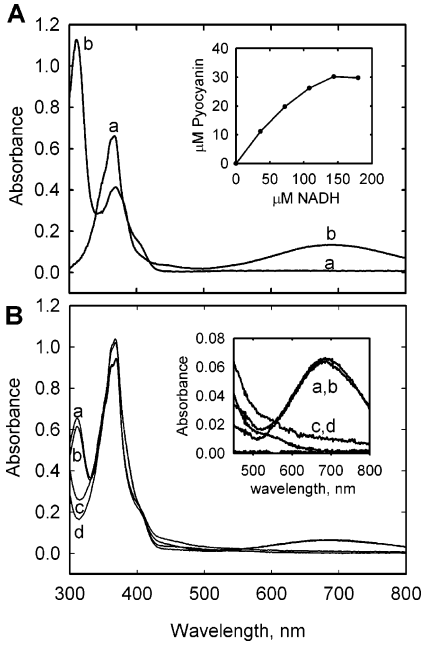

FIGURE 4: Coupled reaction of PhzM and PhzS that converts phenazine-1-caboxylic acid to pyocyanin. Panel A shows spectra observed prior to the addition of NADH (a) and subsequent to titration with NADH (b). Typical absorption of PCA in pH 7.8 reaction buffer at 370 nm is observed prior to NADH addition, while typical absorption of pyocyanin at 310, 370, and 690 nm (broad) is observed at the end of the reaction. Wavelengths of <300 nm are obscured by absorbance of the PhzM cofactor, *S*-adenosylmethionine, and its reaction products. The inset is a plot of pyocyanin production vs NADH consumption for the reaction, indicating that more than stoichiometric amounts of NADH were required to approach total conversion of PCA in the reaction (34 μM) to pyocyanin. Panel B shows the absorption spectra of reactions carried out in equilibrium dialysis chambers separated by 8000 Da molecular mass cutoff dialysis membranes. Spectra a and b were obtained from solutions on separate sides of a chamber that initially had PhzM and PhzS on one side and PCA on the other. Spectra c and d were obtained from solutions on separate sides of a chamber that initially had PhzM and PhzS on opposite sides of the membrane and PCA on both sides. The inset is focused on the absorbance at 690 nm indicative of pyocyanin in samples a and b. Complete conversion of PCA to pyocyanin was not observed in the experiments depicted in panel B due to pyocyanin- and PhzS-mediated oxygen and NADH depletion (see the text).

hydroxylation. Several other compounds, including salicylic acid and gentisic acids, were also determined to uncouple NADH oxidation from substrate hydroxylation. This phenomena has been previously reported for similar enzymes (*26*). To verify, using purified enzymes, previous work suggesting that pyocyanin cannot be produced by methylation of 1-HP, PhzM was assayed for activity toward 1-HP. No pyocyanin production was noted, nor was SAM or 1-HP consumed, indicating 1-HP is not a PhzM substrate or an intermediate in pyocyanin biosynthesis.

When reaction mixtures containing both PhzM and PhzS were analyzed, rapid pyocyanin formation was evident on the basis of the blue color formed in the reaction vessel. Pyocyanin was confirmed and quantitated by its characteristic absorption at 690 nm (Figure 4A). Pyocyanin formation required PhzM, PhzS, PCA, SAM, oxygen, and NADH, consistent with a methyl transfer reaction and a flavin-mediated hydroxylation. Assaying the conversion of PCA to pyocyanin presents unique challenges that have hindered a detailed kinetic analysis thus far. The redox activity of

pyocyanin results in nonenzymatic depletion of NADH and oxygen in assays where pyocyanin is produced. Furthermore, since PCA is an apparently poor substrate for PhzS (and possible inhibitor of pyocyanin formation) and appears to uncouple NADH oxidation from hydroxylation, this consumes more NADH and oxygen and further complicates the kinetic analysis. For example, the inset of Figure 4A shows that complete conversion of 34 μM PCA to pyocyanin required >100 μM NADH.

Evidence for an Interaction between PhzM and PhzS. The observations given above strongly suggested that for PCA to be converted to pyocyanin, an interaction between the two enzymes is required. To confirm this, assays using an equilibrium dialysis cell were conducted. A 350 μL dialysis chamber was assembled with an 8000 Da molecular mass cutoff membrane dividing the chamber in two equal halves. PhzM, SAM, and PCA were placed on one side, while PhzS was placed on the other side, along with NADH. Control experiments with PhzM and PhzS on one side together were also conducted. The chambers were incubated at room temperature for 4−16 h. Analysis of the solutions showed that no pyocyanin was formed when PhzM and PhzS were on opposite sides of the membrane. Pyocyanin was formed when they were on the same side even if all substrates were initially on the other side, indicating that all substrates were able to equilibrate in the chamber (Figure 4B). Larger-scale experiments were conducted to ensure that oxygen depletion in the closed small equilibrium dialysis chambers was not a factor, and these experiments confirmed the results given above. When either enzyme was isolated in a dialysis membrane, no pyocyanin formed in an overnight incubation. The control reaction, with NADH isolated initially, formed pyocyanin within minutes.

Filtration assays also argue that an interaction is required. When reaction mixtures lacking only PhzS were incubated and then filtered to remove PhzM, adding PhzS to the flow-through did not result in any pyocyanin production.

Attempts To Detect a PhzM−PhzS Complex. One possible explanation for the inactivity of PhzM is that a physical interaction with PhzS is required to trigger conversion of PCA to pyocyanin. Laser light scattering experiments were devised to examine whether a stable PhzM−PhzS complex was detectable. Size exclusion chromatography in conjunction with laser light scattering was used to determine the molecular masses of species in mixtures containing PhzM and PhzS in equimolar amounts. No indications of a complex were found. PhzS was determined to have a molecular mass of 42 650 ± 400 Da, indicating it is a monomer in solution (calculated mass of 43926 Da). The entire system was then equilibrated with buffer containing 100 μM SAM, 200 μM NADH, and 400 μM PCA, each alone and in combination, and injections were repeated. Elution profiles and calculated masses did not differ from the data obtained with buffer only in the system, indicating detectable complexes were not formed under these conditions.

DISCUSSION

Pyocyanin was identified in bacterial cultures in the early 1900s, and PCA was long ago identified by Holliman and co-workers as a pyocyanin precursor (*13*). Until recently, however, little was known about the biochemical steps leading to its formation. Genome sequencing and annotation have recently made it possible to predict what gene products might be involved in a given biochemical process. Mavrodi et al. (*12*) proposed that PhzM and PhzS were responsible for converting PCA to pyocyanin in *P. aeruginosa*. Knocking out either gene resulted in cultures that could not produce pyocyanin. When *phzM* was deleted, 1-HP accumulated in cultures, and when *phzS* was deleted, an unidentified, red, water soluble pigment was produced. Previously, it had been suggested that 1-HP was not a pyocyanin precursor which led to the proposal that the putative methylase PhzM acted first on PCA to produce 5-MePCA which was then converted to pyocyanin by the putative hydroxylase PhzS. To systematically characterize pyocyanin formation in vitro, a structural and biochemical analysis of PhzM and PhzS was undertaken.

The crystal structure of PhzM is consistent with it being a small molecule methyltransferase. The structure exhibits the α/β-hydrolase-like SAM binding domain that is characteristic of methyltransferases. There are two notable aspects to the structure of PhzM, the dimer interface and the exposed active site relative to other methyltransferases. The intertwined helix motif that forms the interface is seen in only a few other methyltransferase structures, four from plants and three from bacteria (Table 3). In the plant enzymes, the dimer interface contributes one wall of the substrate binding site with residues from the N-terminal region (domain I) of one subunit protruding into the active site of the second subunit. It was proposed that variability in the residues contributed by the opposite subunit may be a mechanism by which plant methyltransferases dictate substrate selectivity (*16*). In the bacteriochlorophyll biosynthetic enzyme BchU, residues from both subunits also contribute to substrate binding (*27*). It is unknown yet whether this is a factor in binding of PCA to PhzM, but it is apparent that PCA likely binds in an orientation different (by ~90°) than that seen for isoformononetin in the isoformononetin−IOMT complex (1FP2), for example, since isoformononetin (also a tricyclic compound) is methylated on an oxygen at the end of its long axis while PCA is methylated at N5 in the center of the molecule. This may place PCA too far from that surface of the active site for any contacts to be made.

The active site of PhzM, as shown in Figures 3, is solvent-exposed in the unliganded state. Attempts to obtain a structure of PhzM with bound substrates or products have thus far been unsuccessful. Experiments employing the crystallization conditions described above yielded few crystals when one or more possible ligands were included, and screening indicated that those that did grow were unliganded. Soaking experiments were also unsuccessful. One possibility is that the crystal lattice will not accommodate ligands and that new crystallization conditions will need to be identified when ligands are present. Such efforts have not yet been successful. Another possibility is that the observed structure represents accurately the state of PhzM in solution and that the protein is in an inactive state until a transition to an active state is triggered. The PhzM-catalyzed reaction is expected to occur via nucleophilic attack by the lone electron pair of N5 of PCA on the reactive sulfonium methyl group of SAM (*23*). Unlike reactions catalyzed by homologous *O*-methyltransferases, the PhzM-catalyzed reaction does not require a base-assisted deprotonation step to generate a nucleophile (*16*). Therefore, it is expected that PhzM primarily enhances

the reaction rate by bringing the substrates together in the proper orientation for catalysis. DnrK methyltransferase (Table 3) was proposed to operate in a similar manner despite catalyzing an O-methylation (*28*). When the putative catalytic base of DnrK was mutated, the enzyme retained nearly 50% activity, suggesting that other factors play large roles in catalysis.

As described above, PhzM alone appears inactive unless PhzS is also present. This suggests that PhzS is able to trigger a change that renders PhzM active. The data from the dialysis experiment (Figure 4) and the filter assays suggest that an at least transient physical interaction between PhzM and PhzS is required for pyocyanin formation to occur. Interestingly, the PhzM homologue, IOMT from alfalfa (Table 3), has also been proposed to form a complex in vivo (*16*, *29*). Evidence suggests that IOMT may interact with isoflavanone synthase possibly to ensure synthesis of a particular isoflavanoid. *P. aeruginosa* may be employing a similar strategy to ensure the synthesis of pyocyanin. It was previously demonstrated that 5-Me-PCA is the apparent precursor not only to pyocyanin but also to another pigment, aeruginosin A [7-amino-5-methylphenazine-1-carboxylate (*13*)]. The biosynthetic pathway leading to aeruginosin A is uncharacterized, but the results presented here for pyocyanin biosynthesis suggest that *P. aeruginosa* has developed mechanisms that regulate the partitioning of this common intermediate. Ongoing experiments using inactive variants of PhzS and the development of a synthetic route for the putative intermediate should permit a detailed assessment of the nature of the apparent interaction between PhzM and PhzS.

REFERENCES

1. Laursen, J. B., and Nielsen, J. (2004) Phenazine Natural Products: Biosynthesis, Synthetic Analogues, and Biological Activity, *Chem. Rev. 104*, 1663−1686.
2. Lau, G. W., Ran, H., Kong, F., Hassett, D. J., and Mavrodi, D. (2004) *Pseudomonas aeruginosa* pyocyanin is critical for lung infection in mice, *Infect. Immun. 72*, 4275−4278.
3. Van Delden, C., and Iglewski, B. H. (1998) Cell-to-cell signaling and *Pseudomonas aeruginosa* infections, *Emerging Infect. Dis. 4*, 551−560.
4. Zelenitsky, S. A., Harding, G. K., Sun, S., Ubhi, K., and Ariano, R. E. (2003) Treatment and outcome of *Pseudomonas aeruginosa* bacteraemia: An antibiotic pharmacodynamic analysis, *J. Antimicrob. Chemother. 52*, 668−674.
5. Reszka, K. J., Denning, G. M., and Britigan, B. E. (2006) Photosensitized oxidation and inactivation of pyocyanin, a virulence factor of *Pseudomonas aeruginosa*, *Photochem. Photobiol. 82*, 466−473.
6. Lau, G. W., Hassett, D. J., Ran, H., and Kong, F. (2004) The role of pyocyanin in *Pseudomonas aeruginosa* infection, *Trends Mol. Med. 10*, 599−606.
7. Mavrodi, D. V., Ksenzenko, V. N., Bonsall, R. F., Cook, R. J., Boronin, A. M., and Thomashow, L. S. (1998) A seven-gene locus for synthesis of phenazine-1-carboxylic acid by *Pseudomonas fluorescens* 2-79, *J. Bacteriol. 180*, 2541−2548.
8. Parsons, J. F., Calabrese, K., Eisenstein, E., and Ladner, J. E. (2003) Structure and mechanism of *Pseudomonas aeruginosa* PhzD, an isochorismatase from the phenazine biosynthetic pathway, *Biochemistry 42*, 5684−5693.
9. Blankenfeldt, W., Kuzin, A. P., Skarina, T., Korniyenko, Y., Tong, L., Bayer, P., Janning, P., Thomashow, L. S., and Mavrodi, D. V. (2004) Structure and function of the phenazine biosynthetic protein PhzF from *Pseudomonas fluorescens*, *Proc. Natl. Acad. Sci. U.S.A. 101*, 16431−16436.
10. Parsons, J. F., Song, F. H., Parsons, L., Calabrese, K., Eisenstein, E., and Ladner, J. E. (2004) Structure and Function of the Phenazine Biosynthesis Protein PhzF from *Pseudomonas fluorescens* 2-79, *Biochemistry 43*, 12427−12435.
11. Parsons, J. F., Calabrese, K., Eisenstein, E., and Ladner, J. E. (2004) Structure of the phenazine biosynthesis enzyme PhzG, *Acta Crystallogr. D60*, 2110−2113.
12. Mavrodi, D. V., Bonsall, R. F., Delaney, S. M., Soule, M. J., Phillips, G., and Thomashow, L. S. (2001) Functional analysis of genes for biosynthesis of pyocyanin and phenazine-1-carboxamide from *Pseudomonas aeruginosa* PAO1, *J. Bacteriol. 183*, 6454−6465.
13. Hansford, G. S., Holliman, F. G., and Herbert, R. B. (1972) Pigments of *Pseudomonas* species. Part IV. In vitro and in vivo conversion of 5-methylphenazinium-1-carboxylate into aeruginosin A, *J. Chem. Soc., Perkin Trans. 1*, 103−105.
14. Flood, M. E., Herbert, R. B., and Holliman, F. G. (1972) Pigments of *Pseudomonas* Species. Part V. Biosynthesis of Pyocyanin and the Pigments of *Ps. aureofaciens*, *J. Chem. Soc., Perkin Trans. 1*, 622−626.
15. Frank, L. H., and DeMoss, R. D. (1959) On the Biosynthesis of Pyocyanine, *J. Bacteriol. 77*, 776−782.
16. Zubieta, C., He, X. Z., Dixon, R. A., and Noel, J. P. (2001) Structures of two natural product methyltransferases reveal the basis for substrate specificity in plant O-methyltransferases, *Nat. Struct. Biol. 8*, 271−279.
17. Pflugrath, J. W. (1999) The finer things in X-ray diffraction data collection, *Acta Crystallogr. D55*, 1718−1725.
18. Sheldrick, G. M. (1998) in *Direct Methods for Solving Macromolecular Structures* (Dordrecht, F. S., Ed.) pp 401−411, Kluwer Academic Publishers, Dordecht, The Netherlands.
19. Terwilliger, T. C. (2003) Automated main-chain model building by template matching and iterative fragment extension, *Acta Crystallogr. D59*, 38−44.
20. Winn, M., Isupov, M., and Murshudov, G. N. (2001) Use of TLS Parameters to Model Anisotropic Displacements in Macrololecular Refinement, *Acta Crystallogr. D57*, 122−133.
21. Gurusiddaiah, S., Weller, D. M., Sarkar, A., and Cook, R. J. (1986) Characterization of an Antibiotic Produced by a Strain of *Pseudomonas fluorescens* Inhibitory to *Gaeumannomyces graminis* var. *tritici* and *Pythium* spp., *Antimicrob. Agents Chemother. 29*, 488−495.
22. Halaka, F. G., Babcock, G. T., and Dye, J. L. (1982) Properties of 5-Methylphenazinium Methyl Sulfate, *J. Biol. Chem. 257*, 1458−1461.
23. Schubert, H. L., Blumenthal, R. M., and Cheng, X. (2003) Many paths to methyltransfer: A chronicle of convergence, *Trends Biochem. Sci. 28*, 329−335.
24. Kawabata, T. (2003) MATRAS: A program for protein 3D structure comparison, *Nucleic Acids Res. 31*, 3367−3369.
25. Takata, Y., Huang, Y., Komoto, J., Yamada, T., Konishi, K., Ogawa, H., Gomi, T., Fujioka, M., and Takusagawa, F. (2003) Catalytic mechanism of glycine N-methyltransferase, *Biochemistry 42*, 8394−8402.
26. Tsuji, H., Ogawa, T., Bando, N., and Sasaoka, K. (1986) Purification and properties of 4-aminobenzoate hydroxylase, a new monooxygenase from *Agaricus bisporus*, *J. Biol. Chem. 261*, 13203−13209.
27. Wada, K., Yamaguchi, H., Harada, J., Niimi, K., Osumi, S., Saga, Y., Oh-Oka, H., Tamiaki, H., and Fukuyama, K. (2006) Crystal structures of BchU, a methyltransferase involved in bacteriochlorophyll c biosynthesis, and its complex with S-adenosylhomocysteine: Implications for reaction mechanism, *J. Mol. Biol. 360*, 839−849.
28. Jansson, A., Koskiniemi, H., Mantsala, P., Niemi, J., and Schneider, G. (2004) Crystal structure of a ternary complex of DnrK, a methyltransferase in daunorubicin biosynthesis, with bound products, *J. Biol. Chem. 279*, 41149−41156.
29. Liu, C.-J., and Dixon, R. A. (2001) Elicitor-Induced Association of Isoflavone O-Methyltransferase with Endomembranes Prevents the Formation and 7-O-Methylation of Daidzein during Isoflavanoid Phytoalexin Biosynthesis, *Plant Cell 13*, 2643−2658.

BI6024403